Nonlinear Frequency Response Analysis to Inform Aircraft Control Law Design

Duc H. Nguyen[1], Mark H. Lowenberg[2], and Simon A. Neild[3]
Department of Aerospace Engineering, University of Bristol, Bristol, BS8 1TR

This paper presents the methodology and results of an initial study into generating the nonlinear frequency responses of a longitudinal airliner model – the polynomial NASA GTM – using numerical continuation with periodic forcing. The results are compared with the linear frequency responses to inform control designers of the extent to which a linearized model can adequately capture the system behavior in the frequency domain. Since the aerospace industry typically uses linearizations in controller design, both open and closed-loop behaviors are considered. When the aircraft is forced with small elevator deflections, highly nonlinear responses are observed, including period-2 and quasi-periodic motions, as well as subharmonic resonances that lead to loss of stability. Closed-loop responses of a proportional stability augmentation controller become out of phase with the linear prediction at low forcing frequencies when the aircraft operates at high angle of attack. Additionally, two-parameter continuation is used to assess the controller's effectiveness when operated in nonlinear regions where linear controller design techniques cannot be used. Time histories are used to verify the results, which closely follow the nonlinear analysis. To illustrate the concept and validate the method for generating nonlinear frequency response, a brief numerical analysis of the Duffing equation is also presented.

I. Nomenclature

A	=	forcing amplitude (deg or N)
q	=	pitch rate (deg/s)
t	=	time (s)
V	=	total velocity (m/s)
α	=	angle of attack (deg)
Δ	=	incremental, relative to trim value (used as prefix)
δ_e	=	elevator deflection (deg)
θ	=	pitch angle (deg)
γ	=	flight path angle (deg)
ω	=	forcing frequency (Hz or rad/s)
$_o$	=	trim value (used as subscript)

II. Introduction

Aircraft controllers are typically designed using linear techniques at a number of operating points across the flight envelope. The resulting controllers are then combined into a single nonlinear gain-scheduled controller. Although the linear design techniques offer many advantages, most importantly availability of closed-form solutions, this approach may be insufficient when the aircraft operates in highly nonlinear regions. This is a problem during extreme maneuvering in a fighter aircraft, or in upsets and loss-of-control situations in a civilian aircraft. Therefore, it is important to determine the extent to which the linear model can capture the dynamics before the predicted response

[1] PhD student, Department of Aerospace Engineering, Student Member AIAA.
[2] Professor of Flight Dynamics, Department of Aerospace Engineering, Senior Member AIAA.
[3] Professor of Nonlinear Structural Dynamics, Department of Aerospace Engineering.

no longer adequately matches the actual response on the full nonlinear model. This paper proposes a novel approach to study this problem. In particular, the numerical tools from bifurcation analysis are utilized to capture the nonlinear behavior of the system coupled with a harmonic oscillator, which permits the assessment of frequency-domain-based assumptions used in linear control design, such as stability margins or superposition. The objective is to inform the control designer of regions in which linear-based design is insufficient.

Nonlinear phenomena in flight dynamics have been widely documented, and much research has been done to combine nonlinear analysis with classical flight dynamics and control theory to improve performance and safety. Since their first application on an aircraft model [1], bifurcation analysis and continuation methods have gained recognition in the flight dynamics research community as a powerful tool in studying nonlinear phenomena at high angle of attack commonly found in high-performance fighter jets [2-7]. More recently, the tool has been used on civil applications to study airliner upsets and loss-of-control [8-10] following accidents such as Air France flight 447. Specifically, it is shown in [9] that dangerous upset conditions like entry into oscillatory spins caused by an incorrect pilot response from a spiral dive can be characterized as stable attractors in the phase space. A linear representation of the aircraft cannot capture this behavior and as a result, a controller based on this linearization may be unable to recover the aircraft from upsets outside the normal operating envelopes. Indeed, in [10], the analysis was repeated on the same aircraft model coupled with a linear gain-scheduled controller and was successful in identifying upset attractors that are still beyond the controller's capability. Analysis on the effect of controller gains on eliminating those regions of upsets was also done in [10], which proved useful in comparing the robustness of different controller designs.

While most published work on flight dynamics and control using continuation methods focus on studying equilibrium solutions to satisfy handling quality requirements in the time domain, very little has been done to study periodic solutions of a forced system to satisfy frequency-domain criteria. In linear system theory, a harmonic input produces a harmonic output of the same frequency whereas a nonlinear system may have nonharmonic output, i.e. contain multiple frequencies. Moreover, a smooth variation in forcing frequency or amplitude in a linear system produces smooth changes in response amplitude and phase. In a nonlinear system, the resonance peaks are dependent on both frequency and amplitude and may give rise to bistable solutions; a smooth variation in input frequency could then, for example, cause abrupt changes in both amplitude and phase, known as jump phenomena. Forced oscillation of nonlinear systems has been studied in depth, such as in [11-13], but its application has so far been limited to structural engineering [14-17].

Despite limited studies in the flight dynamics context, the problem of nonlinear oscillation can arise in aircraft with complex and highly augmented flight control systems due to coupling between the aircraft's natural modes, structural modes, aerodynamics, and the control system itself. During a series of low altitude and high speed test flights outside the operational envelope, a B-2 encountered residual pitch oscillations in response to a doublet input on control surfaces [18]. The phenomenon was not predicted by analytical methods, wind tunnel tests or previous flutter tests, and subsequent work determined the possible cause to be a complex interaction between transonic aerodynamics and aeroelasticity. The study concluded that a pilot should stay clear of that region in the envelope and made no mention of the B-2's complex and highly classified stability augmentation system, which cannot be disabled in flight [18]. It is possible that the interaction between aerodynamic and structural dynamics had created a highly nonlinear forced oscillation situation, which coupled with the flight control system and led to the pitch oscillation in question. [19] showed that a controller designed on a rigid aircraft model has degraded performance when used on the non-rigid model of the same high aspect-ratio aircraft due to the reduced frequency separation between the rigid-body and flexible modes. Nevertheless, these studies still focus on the structural aspect of the aircraft, and there remains a gap in literature on the topic of nonlinear interactions between the flight control system and the aircraft natural modes. Especially at high angle-of-attack and in regions outside the normal operational envelope, the nonlinear phenomena mentioned above may cause violations of the frequency response criteria, degrade the controller's performance and therefore compromise performance and safety.

Among the few studies on flight dynamics involving forced response using continuation methods are [20, 21]. In [20], a harmonic oscillator is coupled to an F/A-18 model with pilot (modeled as a simple proportional gain) in the loop: the objective was to predict pilot-induced oscillations through observation of rapid increases in output oscillation amplitudes as pilot gain parameter is varied. In [21], the harmonic oscillator was appended to the thrust vector deflection of an F-18 HARV model flying at very high angles of attack, where conventional control surfaces are ineffective. Although the ranges of forcing amplitude and frequency are relatively narrow (no more than 2^o in amplitude and between 0.1 and 1 rad/s in frequency), the aircraft's response is extremely complex. Different combinations of the forcing parameters can result in period-1, period-2, period-4 or chaotic motions caused by a number of period-doubling and torus bifurcations. Moreover, the study also identified the aircraft's sensitivity to initial conditions: given the same forcing parameters, the aircraft's response can be period-1, period-2 or chaotic due to different initial conditions. This is caused by the coexistence of several stable attractors at the same frequencies, some

of which are chaotic and, therefore, give rise to the aircraft's complex behavior. Since a linearization of the model is incapable of capturing these phenomena, knowledge of them is essential to designing an adequate controller, especially for a high-performance aircraft like the F-18 HARV.

This paper expands on the technique presented in [20, 21] to study an aircraft's forced responses, specifically by generating a 'nonlinear Bode plot' to assess the dynamics in the frequency domain. This method is applicable to both open and closed-loop, which can be used to inform the control designer of the controller's validity by comparing its linear and nonlinear frequency responses, thereby determining regions in which the linearized and the full nonlinear model may behave differently. This technique also provides for the possibility of capturing the effects of any unsteady (time-dependent) features in the model - which the evaluation of steady states in an autonomous (unforced) implementation would miss. Before discussing the result of the aircraft model, a similar analysis is applied to the Duffing equation, which is a much simpler system, to present the common phenomena in nonlinear forced systems and to validate the method.

III. Methodology: Bifurcation Analysis of Periodically Forced Systems and a Numerical Analysis of the Duffing Equation

Bifurcation analysis facilitates a systematic study of changes in qualitative behavior of a nonlinear dynamical system. This includes (but is not limited to) the existence of multiple solutions, jump phenomena and stability loss, which are particularly important to flight dynamics. One of the goals of bifurcation analysis is to produce a map of how the system's steady states change with respect to a control parameter (i.e. to construct a bifurcation diagram), and to provide information on the nature and stability of those solutions. This process requires solving the full nonlinear equations of motion of the system (such as an aircraft model), which can be very complex analytically. In practice, the equations are usually solved numerically using continuation methods, which utilize a path-following algorithm to trace out the solutions of the system from an initial solution supplied by the user. The varying control parameter in numerical continuation is called the continuation parameter, which can be elevator deflection or center of gravity position in flight dynamics, for example. Bifurcation diagrams do not provide any information on the transient responses, such as how quickly the system converges to a steady state. Therefore, numerical simulations must always be done to verify the results and understand the transient dynamics. More background on bifurcation analysis and continuation methods for autonomous (unforced) systems can be found in [2]. In this paper, bifurcation analysis and continuation methods were implemented in the MATLAB environment using the Dynamical Systems Toolbox [22], which is a MATLAB implementation of the software AUTO [23].

Bifurcation analysis and continuation methods can be extended to periodically-forced systems – the main focus of this paper – and the resulting bifurcation diagrams will be maps of periodic solutions. This can be done by appending a harmonic oscillator in the form of $\sin(\omega t)$ or $\cos(\omega t)$ to the equations of motion by augmenting a system of n states $[x_1, x_2, \dots, x_n]$ with two additional states:

$$\dot{x}_{n+1} = x_{n+1} + \omega x_{n+2} - x_{n+1}(x_{n+1}^2 + x_{n+2}^2) \quad (1)$$
$$\dot{x}_{n+2} = x_{n+2} - \omega x_{n+1} - x_{n+2}(x_{n+1}^2 + x_{n+2}^2) \quad (2)$$

where ω is the forcing frequency in rad/s. It can be shown that $x_{n+1} = \sin(\omega t)$ and $x_{n+2} = \cos(\omega t)$.

To demonstrate this technique along with some of the common phenomena found in a nonlinear periodically forced system, a numerical analysis of the Duffing equation is presented. The Duffing equation is analogous to a mass-spring-damper system with a nonlinear spring. This spring generates a restoring force that is a summation of a term proportional to the linear displacement x and another term proportional to the cubic displacement x^3. The equation can be written as:

$$m\ddot{x} + c\dot{x} + kx + \alpha x^3 = A\cos(\omega t) \quad (3)$$

where t is time in (s), ω is the forcing frequency (rad/s), A is the forcing amplitude (N), α is the nonlinear stiffness coefficient (N/m^3) and the constants m, k and c correspond to mass (kg), linear stiffness (N/m) and damping coefficient (Ns/m), respectively. If α = 0 N/m, equation (3) becomes a linear system with constant stiffness, while α > 0 results in a hardening spring and α < 0 results in a softening spring. Larger magnitude of α leads to a more nonlinear system, which can be shown by examining its frequency response. Consider a specific case:

$$\ddot{x} + 0.2\dot{x} + x + \alpha x^3 = 2.5\cos(\omega t) \quad (4)$$

The system in equation (4) has a natural frequency of 1 rad/s. Figure 1 shows the frequency responses of equation (4) for four different values of α. The stable solutions are shown as solid lines and the unstable solutions are shown as dashed lines. When α is non-zero, the forced response curves bend either to the left side (softening spring) or right side (hardening spring). Figure 2 shows the magnified views of the case $\alpha = 0.05$, corresponding to equation (5).

$$\ddot{x} + 0.2\dot{x} + x + 0.05x^3 = 2.5\cos(\omega t) \tag{5}$$

Due to the effect of nonlinear stiffening spring ($\alpha > 0$), the frequency response of equation (5) leans to the right side, leading to the existence of multiple solutions at certain frequencies, such as at 1.6 rad/s, where three different solutions co-exist. When forced at this frequency, the system will converge to one of the two stable solutions depending on the initial conditions. This can be demonstrated by running a simulated frequency sweep, which forces the system at a slowly increasing or decreasing frequency via a chirp signal. Simulation for increasing ω (Figure 2a) shows a sudden drop in gain and phase near ω = 1.8 rad/s. When ω is decreasing (Figure 2b), an increase in gain and phase is seen around ω = 1.4 rad/s. The system will always follow the stable solutions, and the path it choses depends on the initial conditions, specifically whether the starting point is on the left or right side of the resonance peak. This sensitivity to initial conditions, hysteresis arising from the folding of the solution curve, the existence of multiple solutions, and the subharmonic resonance at low frequencies are distinctive features of a nonlinear system that are absent from a linear system.

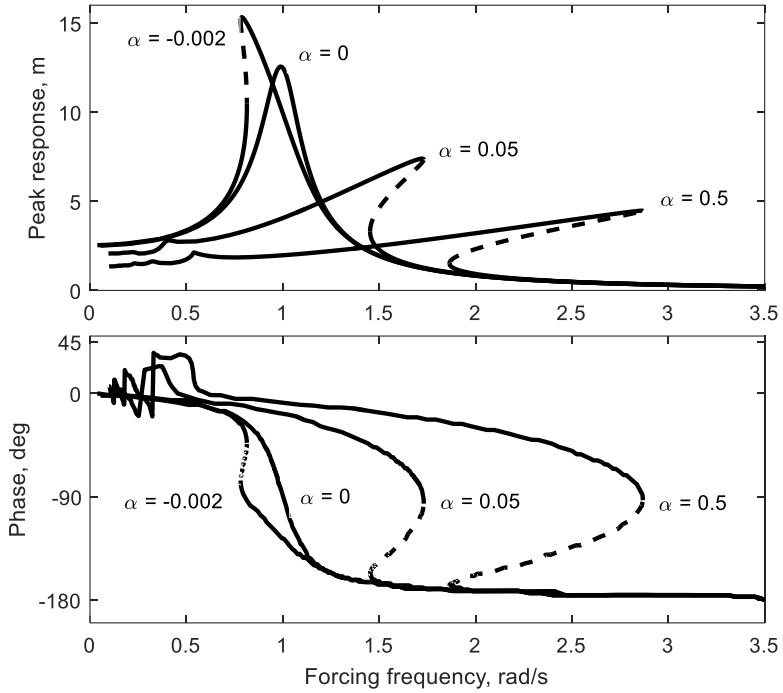

Fig 1 Frequency responses of equation (4) for four different levels of nonlinearity.

The effect of forcing amplitude on the region of multiple solutions is shown in Figure 3: increasing the forcing amplitude makes the system more nonlinear, which widens this region. Using a technique called two-parameter continuation, the locus of the fold bifurcations, where the response curve folds over and leads to the existence of multiple solutions, can be computed. The locus of the fold bifurcations is shown as a thin line in Figure 3, and its projection onto the ω-A plane is shown in Figure 4. It can be seen that if the forcing amplitude is small enough, the fold bifurcations disappear and only one stable solution exists for each forcing frequency, as seen in linear systems. Two-parameter continuation is a powerful technique that can be used to determine a nonlinear region's sensitivity to a system parameter.

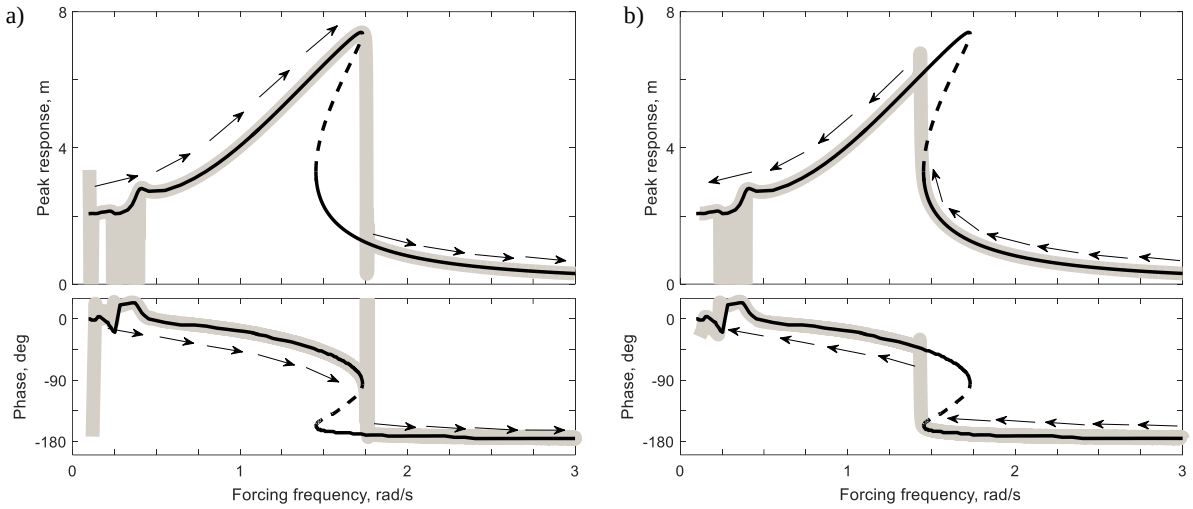

Fig 2 Frequency responses of equation (5) with time-stepping simulated frequency sweeps superimposed (shown in grey). The forcing frequency ω is linearly increasing in (a) and decreasing in (b).

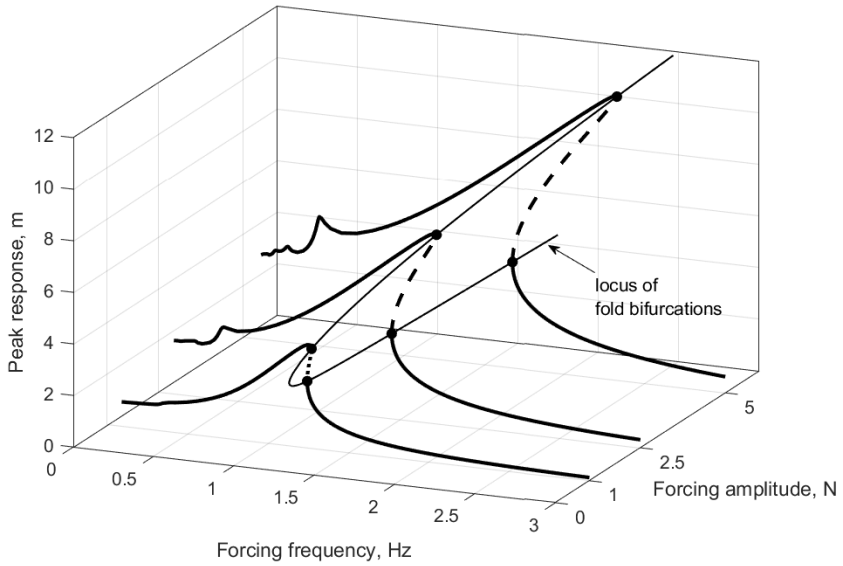

Fig 3 Frequency responses of equation (5) but for three different forcing amplitudes.

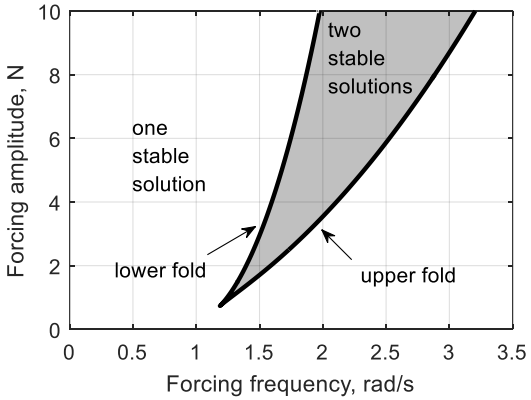

Fig 4 Two-parameter continuation of the fold bifurcation in the ω-A plane.

It is noted that there are some additional small resonances at low frequencies, known as subharmonic resonance, which are more noticeable as the system's nonlinearities become more significant due to increased forcing amplitude. This phenomenon is described in details in [11], and is caused by the existence of additional harmonics in addition to the resonance frequency of 1 rad/s. These harmonics are usually omitted in analytical solutions such as in [13] due to complexity, but can be easily detected using a numerical solver like AUTO. Due to their existence, the simulation has picked up the 'false peaks' shown in Figure 5, which led to the apparent discrepancies between numerical and simulated results shown in Figure 2. In practical terms, this discrepancy is useful in detecting regions where the response is not simply harmonic when examining the simulated frequency response.

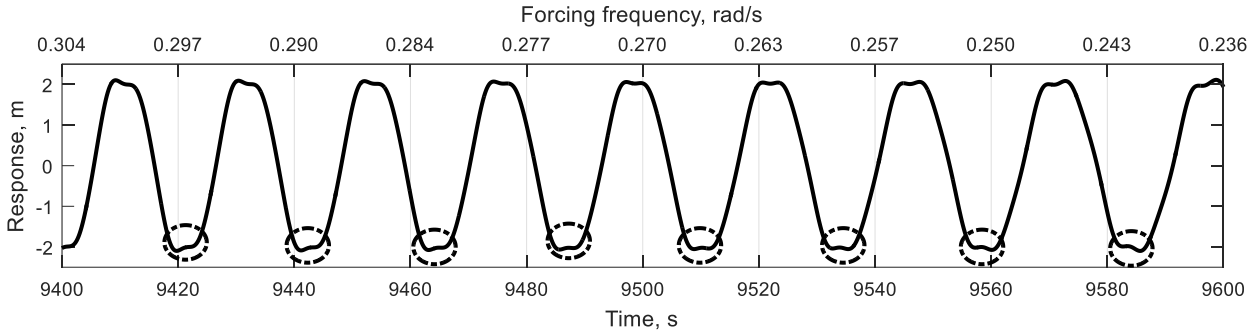

Fig 5 Time histories of the reducing frequency sweep as shown in Figure 2b, showing the crossing of subharmonic resonance region. The 'false peaks' picked up by the code are circled.

The phase diagrams in figures 1 and 2 were constructed by examining the time-domain solution of AUTO for each corresponding forcing frequency. The time-domain solution of equation (5) for two forcing frequencies ω = 2.509 rad/s and ω = 0.298 rad/s are shown in Figure 6. From here, the oscillation amplitude and phase can be computed as follows:

$$amplitude = Y_3 - Y_4 \tag{6}$$

$$phase\ in\ degree = (X_1 - X_3) \times 360 \tag{7}$$

where X_i and Y_i refer to the x and y-coordinates of point i in Figure 6. If a Bode plot is required, the amplitude has to be normalized and converted to decibel:

$$gain = 20\ log_{10}\left(\frac{Y_3 - Y_4}{Y_1 - Y_2}\right) \tag{8}$$

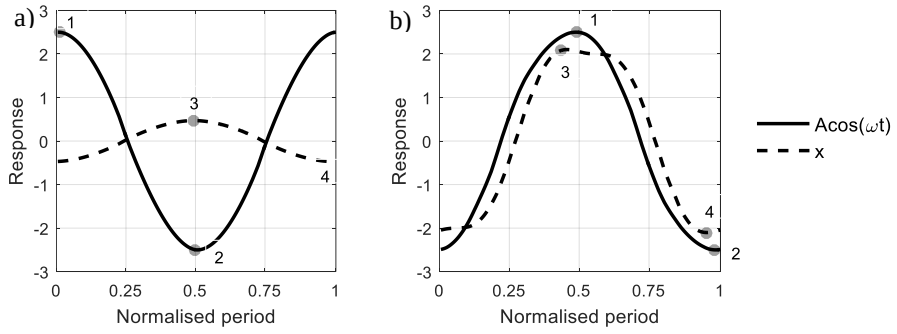

Fig 6 AUTO's solutions to equation (5) for ω = 2.509 rad/s (a) and ω = 0.298 rad/s (b). Points 1 and 3 indicate the forcing peaks and response peaks and points 2 and 4 indicate the forcing troughs and response troughs.

This method of finding the phase is only valid when the response is harmonic. As shown in Figure 6b, the horizontal distance between points 1 and 3 no longer gives the correct physical phase relationship between the input and the output when the response is not simple harmonic. Using this definition of phase, the phase diagram on the frequency response plot should therefore see a small jump at the input frequency for which the output starts to exhibit

a second peak as seen in Figure 2. However, this way of determining the phase is deemed satisfactory as the non-simple-harmonic solutions can be easily identified, which matches the main goal of determining regions where the nonlinear response differs from its linearized counterpart; the latter only produces simple harmonic sinusoidal outputs.

This section has illustrated the types of behavior that a nonlinear system subjected to periodic forcing can produce: subharmonic resonance, frequency and amplitude dependent resonant peaks, bistability and hence hysteresis. The validity of the techniques used on the continuation software AUTO to characterize a simple nonlinear forced system has also been demonstrated. The same techniques were used to analyze the more complex polynomial GTM model, discussed next. In all cases below, the forcing amplitude is fixed at 1°.

IV. Aircraft Model

A polynomial model of the NASA Generic Transport Model (GTM) is used for this study. The GTM is a nonlinear simulation of a 5.5% scale, remotely piloted, generic twin-under-wing engine civil transport aircraft, which was developed to study airliner upsets and loss-of-control. In this paper, a polynomial representation of the GTM [8] is used. This provides the benefits of smooth and differentiable data required for bifurcation analysis and continuation methods, significantly less computational time (at least an order of magnitude faster) and symmetry about the body x-z plane (unlike the full GTM). The version used in this study was originally developed to represent the phugoid instability of the GTM at medium angle of attack, so it is expected that most nonlinearities are to be observed in this region. Because of this, the lateral-directional behavior appears unrealistic: the spiral and roll-subsidence modes combine to form a complex conjugate pair and subsequently move into the right-half plane at medium to high angle of attack (see Figure 7b). For this reason, all the analysis presented here was on the reduced 4th-order model containing only longitudinal states, thereby assuming no lateral and directional motions.

Table 1 lists the two operating points to be studied, which represent medium-high and very high angles of attack. The aircraft is trimmed in straight-and-level flight in all three cases by adjusting the elevator deflection and throttle. This is appropriate as linear gain-scheduled controllers are typically designed around the trim points. The list of symbols used in the nonlinear frequency response is included in Table 2.

Table 1. Operating points of the reduced-order model.

Operating point	$\alpha_0 = \theta_0$ (deg)	V_0 (m/s)	q_0 (deg/s)	δ_{e_0} (deg)	Throttle	Description
1	9	29.6	0	0.68	12.7%	Phugoid mode is marginally damped
2	18	25	0	-7.2	59%	Short period mode is unstable

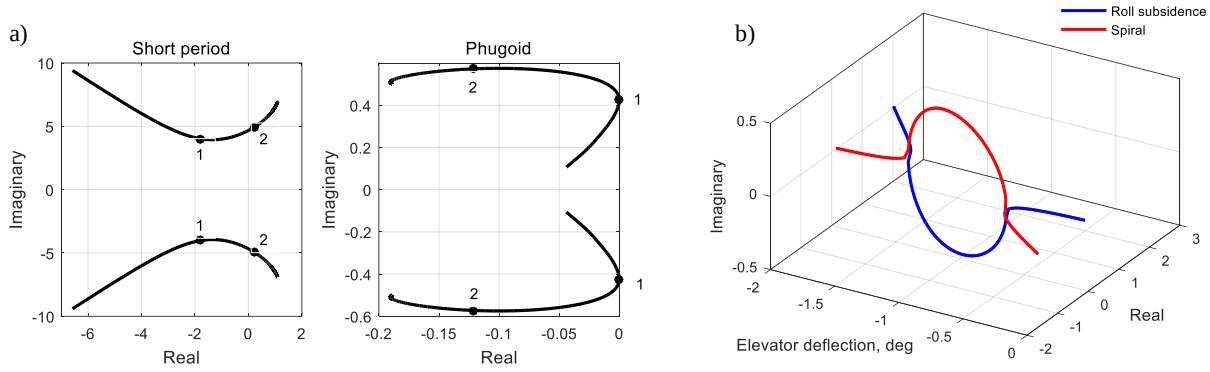

Fig 7 Longitudinal (a) and lateral (b) root loci as the elevator reduces from 6° to the minimum deflection of -30°. The two longitudinal operating points are also highlighted in (a). The Dutch roll mode is not shown in (b) as it is stable throughout and exhibits normal behavior.

Table 2. Notation as used in the nonlinear frequency responses figures and bifurcation diagrams.

———	Stable solution
– – –	Unstable solution
○	Torus bifurcation (the periodically forced response loses stability)
●	Fold bifurcation
□	Period-doubling bifurcation (the forced response repeats itself after twice the forcing cycle)
★	Hopf bifurcation (the unforced response loses stability and enters a limit cycle)

V. Results and Discussions

A. Medium-high angle-of-attack dynamics (α = 9°)

The aircraft is trimmed for straight-and-level flight at 29.6 m/s (see Table 1), corresponding to α = 9°. The open-loop pitch-angle-to-elevator Bode plots are shown in Figure 8 for both the linear and nonlinear model; the latter was obtained by appending equations (1) and (2) to the longitudinal equations of motion, with ω as the continuation parameter. In addition to the two peaks at the phugoid and short-period frequencies (0.07 Hz and 0.60 Hz), the nonlinear model contains additional peaks at low frequencies (between 0.017 and 0.035 Hz) due to the subharmonic resonances as well as a peak at 0.14 Hz (to the right side of the phugoid resonance) due to a pair of period-doubling bifurcations; all of which are not captured in the linear model. Figure 9 shows the magnified views of the subharmonic, phugoid and period-doubling resonance. These regions contain unstable solutions that lead to divergence if the aircraft is forced at one of those frequencies. Moreover, the solution curves lean to the right, indicating that the aircraft resembles a hardening system. The rest of this section will focus on the period-doubling and the subharmonic resonance regions.

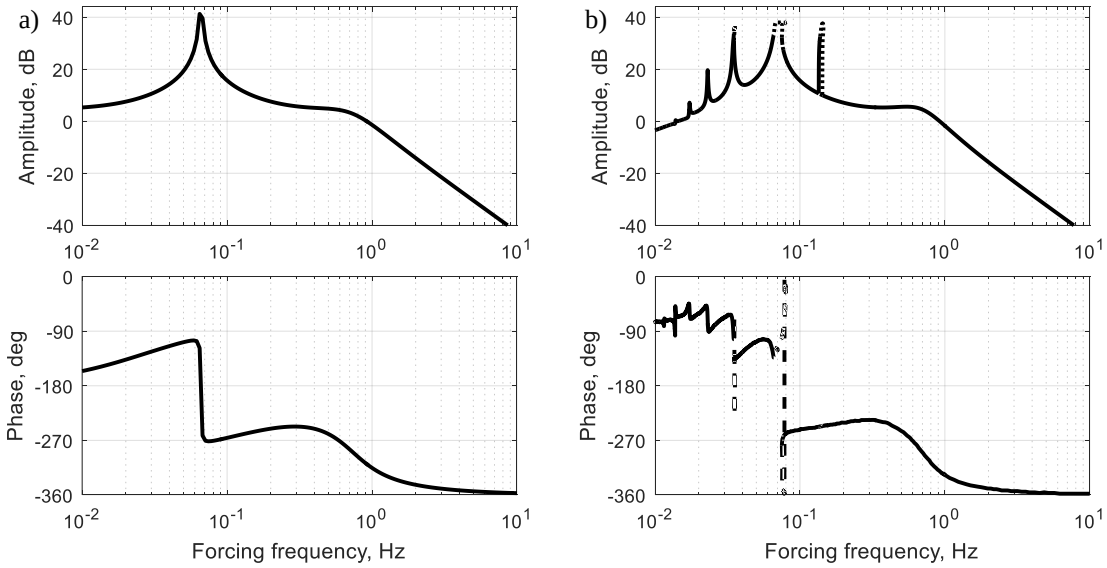

Fig 8 Linear (a) and nonlinear (b) open-loop pitch-angle-to-elevator Bode plots at α = 9°. The bifurcation symbols in (b) are not shown for clarity.

Figure 10 shows the silmulation results when the aircraft is forced at 0.137 Hz and 0.138 Hz (the two unlabelled vertical grids in Figure 9c), which lie between the period-doubling bifurcations. The former is a stable solution and the latter is an unstable solution, which are separated by a torus bifurcation. In both cases, the motion repeats itself after two forcing cycles instead of one, and the oscillation amplitude is very large comparing to the linear model's perediction. If the forcing frequency lies within the unstable region such as in the second case (0.138 Hz), the aircraft diverges. This large amplitude period-2 motion is undesirable. Suppose a proportional pitch-angle-feedback controller is used, it is not possible to rely on linear design techniques to determine the controller's effectiveness in eliminating the period-2 region as this motion is not captured by the linear model. Instead, the two-parameter continuation technique can be used. By setting the controller gain and forcing frequency as the first and second parameters, the relationship between controller gain and the size of the period-2 region can be determined. This is shown in Figure

11. As the controller gain increases, the two period-doubling bifurcations approach each other, reducing the size of the period-2 region, and finally merge when the controller gain reaches 0.01379, meaning that this is the minimum gain required to eliminate the period-2 motion. To verify this, the aircraft is forced again at 0.138 Hz but with the gain set at 0.0140, shown in Figure 12. Comparing to Figure 10b, the oscillation is now stable and has the same period as the forcing term, confirming that the period-doubling bifurcations no longer exist in the main solution branch.

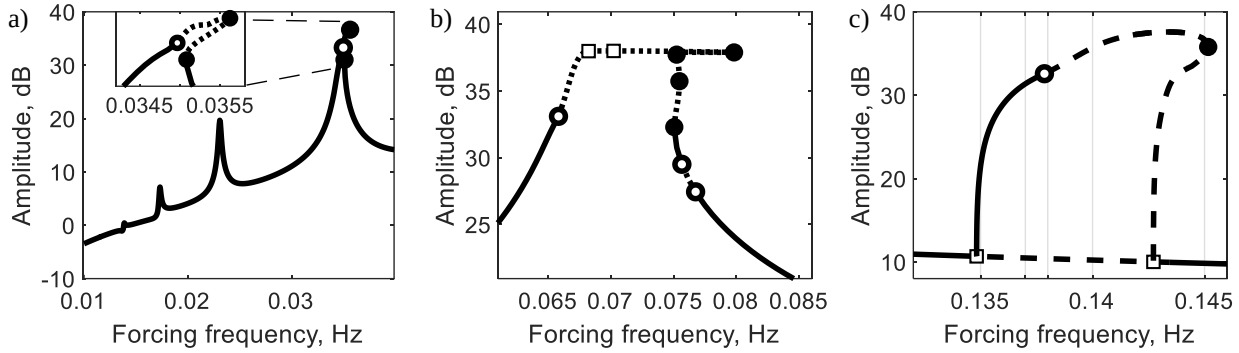

Fig 9 Magnified view of the subharmonic resonances (a), phugoid resonance (b) and period-2 region.

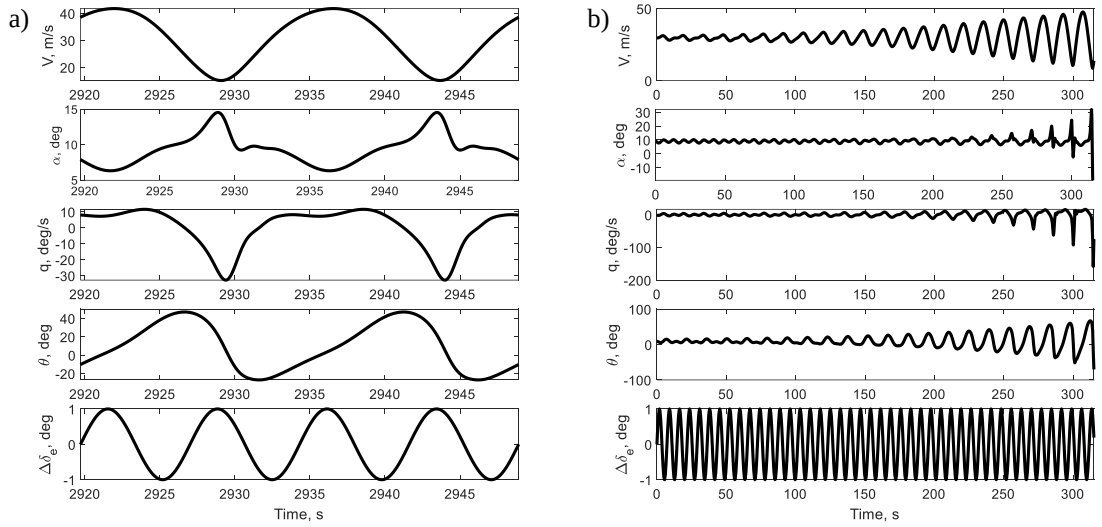

Fig 10 Simulation of the open-loop aircraft forced at 0.137 Hz (a) and 0.138 Hz (b), showing period-2 motions.

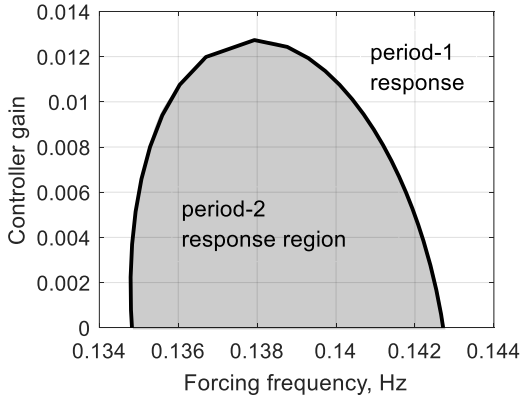

Fig 11 Locus of the period-doubling bifurcations obtained using two-parameter continuation.

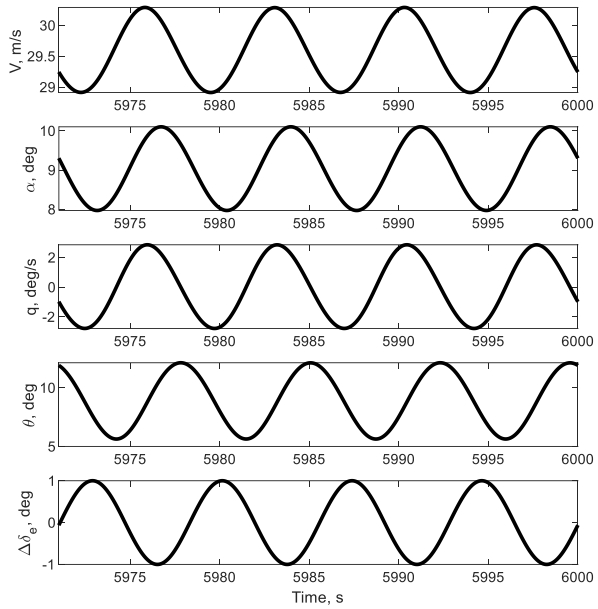

Fig 12 Simulation of the closed-loop aircraft forced at 0.138 Hz with controller gain at 0.014.

The two-parameter continuation is further utilized for the subharmonic resonance region. Figure 13 shows the magnified frequency response at the highest subharmonic peak for three different controller gains (note the change of unit on the y-axis from normalized amplitude in dB to peak response in degree), and Figure 14 shows their 3D projections. As the controller gain increases, the unstable region at the peak of the subharmonic resonance near 0.035 Hz reduces in size and eventually 'detaches' from the main solution branch, forming an isola, which becomes even smaller and moves away from the main branch as the gain increases further (not shown). Although the isola is not connected to the main solution branch by definition, making it difficult to be detected using numerical continuation, it is still possible to do so by tracking the movement of the fold bifurcations in the two parameter space, as shown here in figures 14 and 15. The movement of the torus bifurcation can also be used as a guide: as the gain increases, the torus and the lower fold bifurcations approach each other and eventually merge as the unstable region detaches from the main branch. Beyond this point, the torus bifurcation disappears and the two fold bifurcations move further away, forming the isola. Finally, time simulation is used to verify the effect of the controller at removing the unstable region. Figure 16 shows the aircraft's responses to elevator forcing at 0.03503 Hz, which lies within the unstable region of the subharmonic resonance shown in Figure 13. In the first two cases (open-loop and at gain $4.0\text{x}10^{-4}$), the unstable region is still attached to the main branch and the aircraft diverges. However, at gain $4.6\text{x}10^{-4}$, the response is bounded and stable as the unstable region is no longer linked to the main branch. In principle, the presence of the isola can influence dynamic response in this region, e.g. in the case of a large pitch disturbance. Similar to the period-doubling region, the subharmonic resonance is not captured by the linear model, so it is not possible to use linear design technique to assess the controller's effectiveness in controlling the subharmonic resonance.

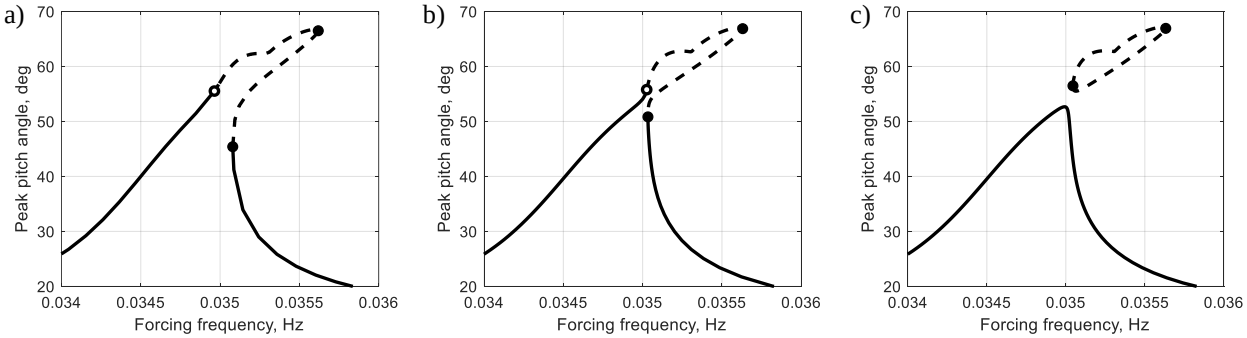

Fig 13 Frequency response at the highest subharmonic peak for three different controller gains: 0 (a), $4.0\text{x}10^{-4}$ (b), and $4.6\text{x}10^{-4}$ (c).

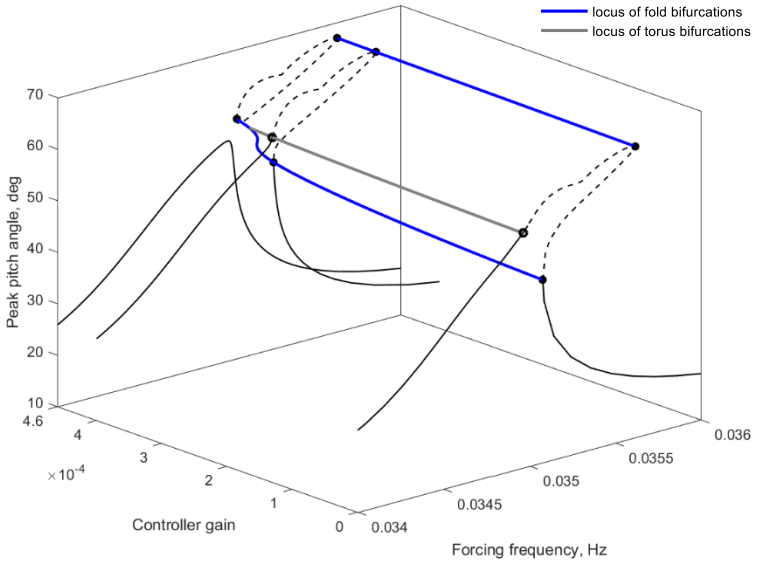

Fig 14 3D projection of Figure 13.

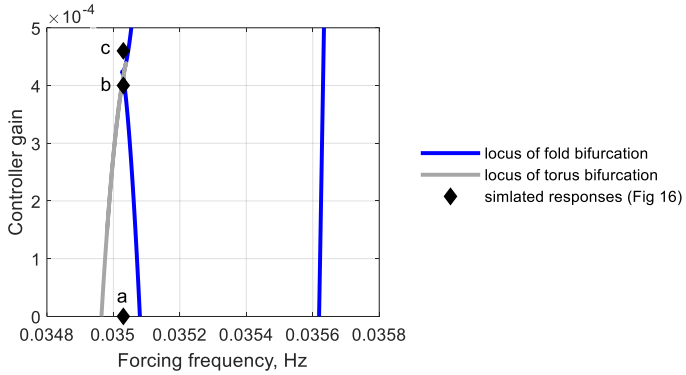

Fig 15 Two-parameter continuation of the fold and torus bifurcation at the highest subharmonic peak.

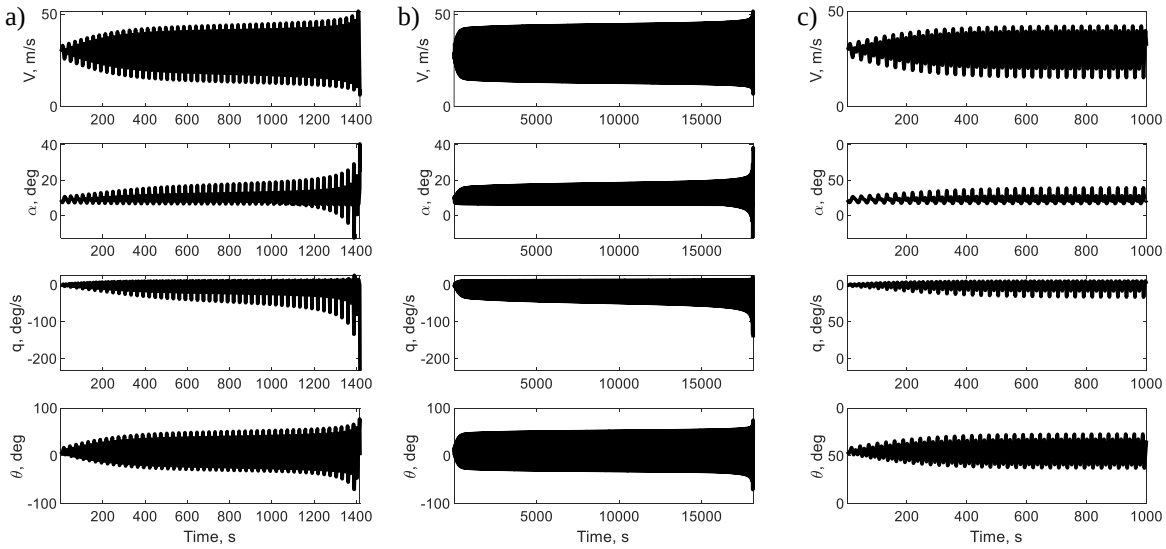

Fig 16 Simulated response of the aircraft forced at 0.03503 Hz for three controller gains: 0 (a), 4.0x10^{-4} (b), and 4.6x10^{-4} (c).

This section has shown the advantages of using nonlinear analysis in identifying the undesirable dynamics in the frequency domain that are not captured by the linear model. Moreover, the two-parameter continuation has been used to assess the controller's effectiveness in removing those undesirable attractors. At the time of writing, the period-two and subharmonic regions have also been observed in the full NASA GTM, and the two-parameter continuation has been successfully applied to identify how to supress the period-two motion. It is also possible to extend the technique to time domain to trace the movements of the undesirable isolas observed in [10]. This use of two-parameter continuation in the time domain is briefly discussed at the end of section B.

B. Very high angle-of-attack dynamics ($\alpha = 18^o$)

The aircraft is trimmed for straight-and-level flight at $\alpha = 18^o$ (see Table 1). Since the short-period mode is unstable at this angle of attack, the unforced aircraft enters a limit cycle – a self-sustaining bounded oscillation – without any external input. Forcing the open-loop aircraft at this angle-of-attack will resulting in quasi-periodic motion shown in figures 17b and 18. On the other hand, the linear model cannot capture this behavior and can only indicate that the aircraft is unstable. Therefore, the linear aircraft diverges as soon as it is perturbed from the trim condition, whether forced or unforced (the former is shown in Figure 17a). Since the linear stability criteria in the frequency domain only applies when the open-loop plant is stable, the open-loop frequency response is not considered here.

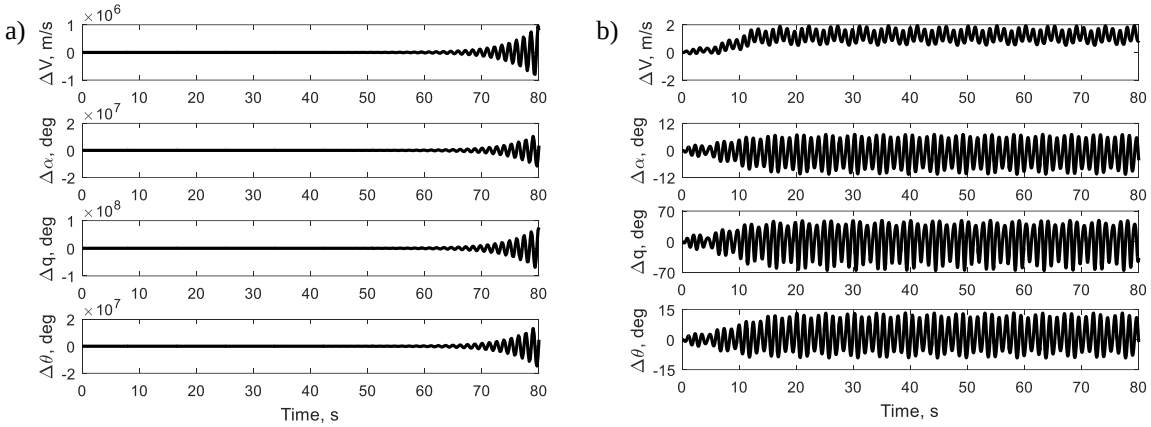

Fig 17 Linear (a) and nonlinear (b) open-loop aircraft responding to an elevator forcing at 1 Hz.

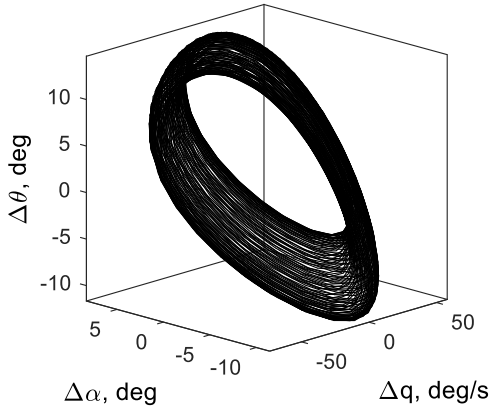

Fig 18 Phase plot of the open-loop aircraft responding to an elevator forcing at 1 Hz, showing bounded quasi-periodic motion. The initial transition motion has been removed from the figure.

To stabilize the short-period mode, a q-feedback stability augmentation controller with proportional gain 0.05 is used. Figure 19 compares the linear and nonlinear closed-loop unforced responses when subjected to an elevator perturbation of 0.1° and duration 0.1s. Whilst the short-period responses are similar, it can be seen that the phugoid mode is much less damped in the nonlinear model. This feature is more prominent in the frequency domain. Figure 20 compares the linear and nonlinear closed-loop frequency responses, where large discrepancies are seen at low frequencies. In particular, a large difference in gain and phase is observed around the phugoid frequency near 10^{-1} Hz.

As the forcing frequency is reduced further, the gain becomes similar again while the phase difference increases to as high as 180º. This means that at low frequencies, the nonlinear pitch angle response is completely out of phase with the linear model and hence with the pilot input. To verify this, the linear and nonlinear models are simulated with a harmonic elevator input of magnitude 1º and frequency 0.07358 Hz (Figure 21). This frequency was chosen as it is near the peak of the phugoid resonance, where largest discrepancies in gain are observed between the linear and nonlinear models. It can be seen that although the controller has stabilized the aircraft, the response it is completely out of phase at low frequencies. This leads to degraded handling qualities and is not captured by the linear model.

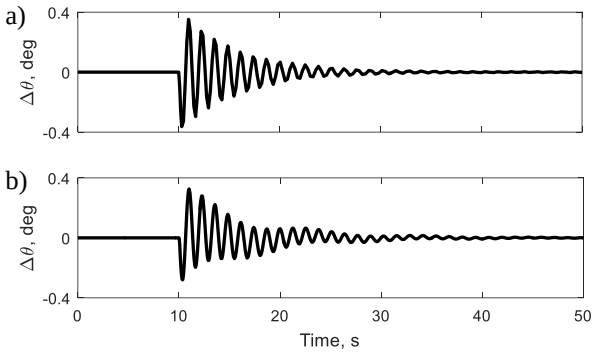

Fig 19 Linear (a) and nonlinear (b) closed-loop aircraft responding to an elevator perturbation.

It has been shown that the phugoid mode leads to the discrepancies between the linear and nonlinear forced responses. In the rest of this section, the effect of the phugoid mode in the aircraft dynamics is investigated by applying the two-parameter continuation in the time domain (on the unforced aircraft). Figure 22 shows the unforced bifurcation diagrams of the trimmed aircraft for angles-of attack ranging from 2.3º to 24.2º – the upper limit is due to the elevator's maximum travel range of ±30º. In the open-loop case (Figure 22a), the aircraft is unstable at $\alpha = \theta = 18^{o}$ due to a Hopf bifurcation at a slightly lower angle-of-attack, which destabilizes the short-period mode and leads to the birth of the limit cycle. Adding the q-feedback controller with proportional gain 0.05 raises the maximum stable angle-of-attack to 19.6º (Figure 22b), which includes the 18º operating point. However, the controller destabilizes the phugoid mode at lower angles-of-attack, shown by the birth of two Hopf bifurcations that create an unstable region for α between 7.5º and 11.5º. Although this effect is reflected in the linear model's root locus of the phugoid mode (Figure 23), it has been shown in Figure 19 that the phugoid destabilization is not adequately captured in the linear model's response to an elevator perturbation.

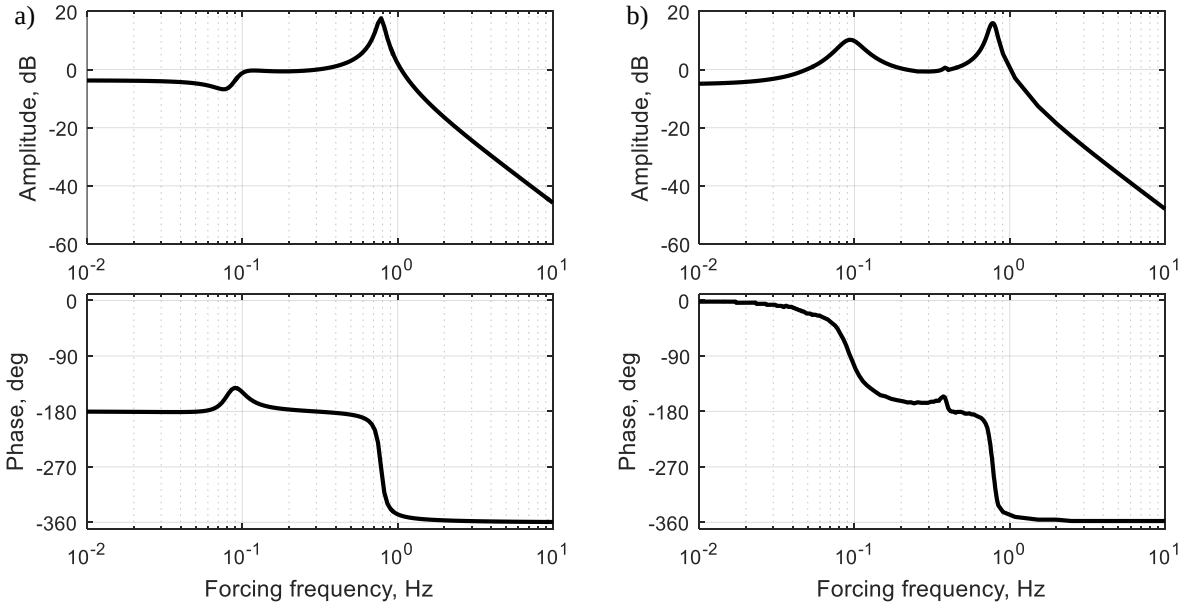

Fig 20 Linear (a) and nonlinear (b) closed-loop pitch-angle-to-elevator Bode plots.

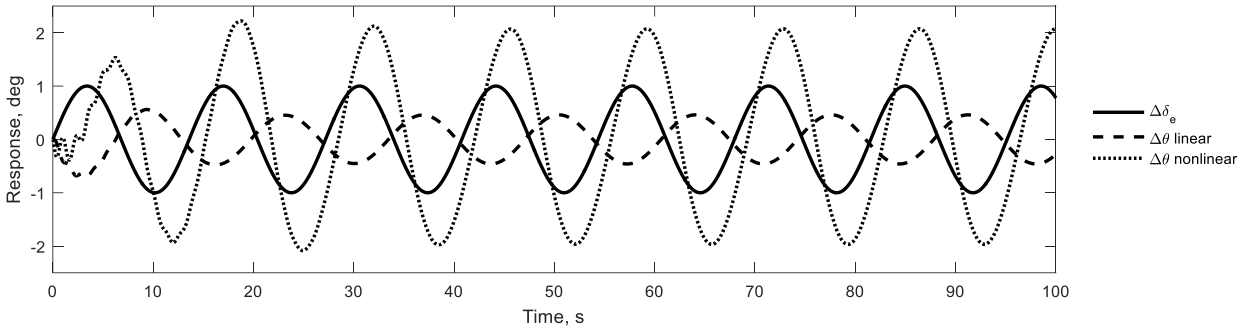

Fig 21 Time histories of the closed-loop linear and nonlinear models responding to an elevator forcing of 1º at 0.07358 Hz.

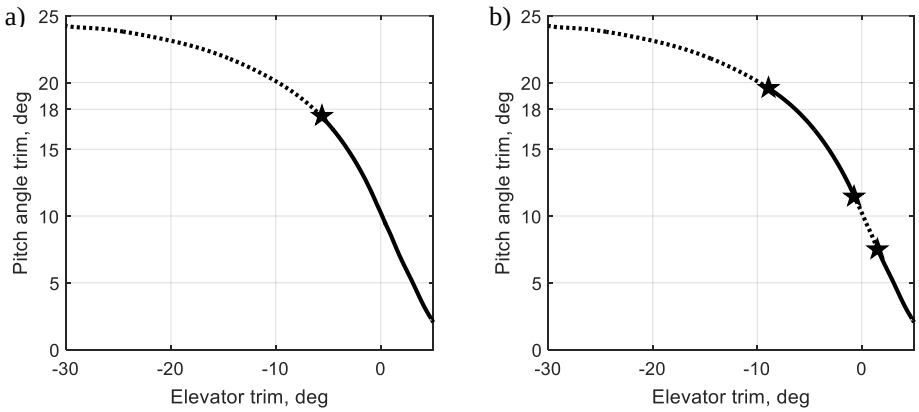

Fig 22 Bifurcation diagram of the trimmed and unforced aircraft without the controller (a) and with the q-feedback controller with gain 0.05 (b).

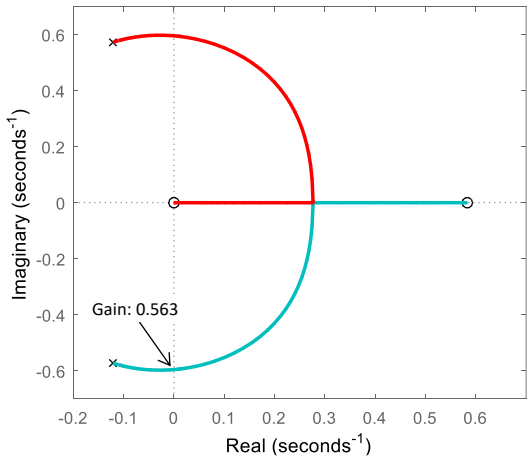

Fig 23 Root locus of the phugoid mode with the proportional q-feedback controller at $\alpha = 18^{o}$.

Two-parameter continuation is now used to trace the locus of the Hopf bifurcation as a function of controller gain. The result in Figure 24 shows that although the unstable short-period region rapidly reduces in size as the controller gain increases, the unstable phugoid region increases in size. Using this technique, a range of controller gains that ensures the aircraft remains stable can be generated. In this example, the range of gains that stabilizes the aircraft from the locus of the Hopf bifurcation matches the root locus. Further inspection of the magnified view shows that although the elevator does not cross into any unstable region as shown in the forced response in figures 20b and 21, the gain and phase discrepancies at low frequencies comparing to the linear response may be attributed to the destabilization of the phugoid mode in the background.

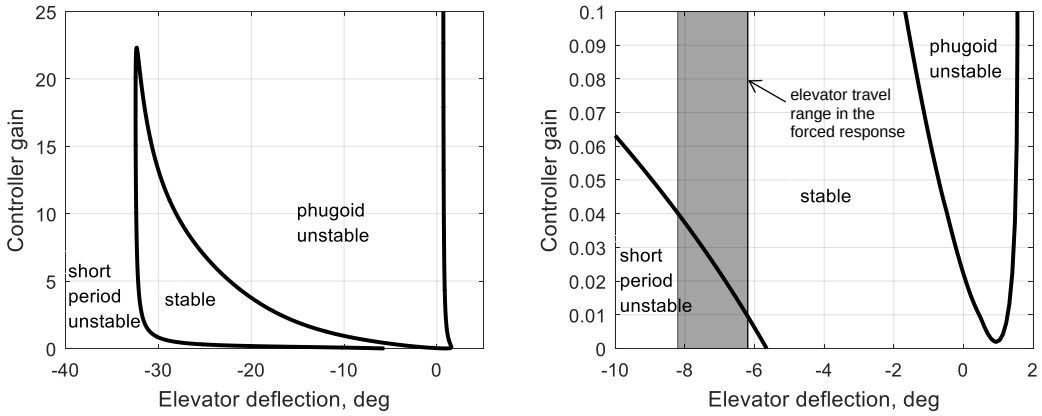

Fig 24 Two-parameter continuation of the Hopf bifurcation. The second figure shows the magnified view near the operating point of δ_e = -7.15º ($\alpha = \theta$ = 18º) and gain 0.05.

This section has presented an example in which the linear model cannot adequately capture the aircraft dynamics. The use of closed-loop forced response and two-parameter continuation have been shown to be useful in informing the control designer of the lack of robustness of the controller in both the frequency and time domains.

VI. Conclusion

This paper has presented methods of understanding the full nonlinear frequency responses of an aircraft model using numerical continuation. It has been shown that the technique gives a clear indicator of where the behavior of the linearized model may differ significantly from that of the full model. The technique is applicable to both open and closed-loop analysis. Classical controller design methods rely on linearized models, which do not capture all the dynamics, especially at high angles of attack or during rapid maneuvering where nonlinearity becomes significant. On the other hand, the use of two-parameter continuation with controller gain proved useful in determining the controller's effectiveness in eliminating the undesirable attractors that either degrade the aircraft's handling qualities or lead to dynamics that are completely uncaptured by the linear model. Therefore, the information gained from the nonlinear frequency response will help determine whether the controller performs as predicted when implemented on the nonlinear model. The adoption of a periodically forced bifurcation and continuation method approach also allows the contributions of any time-dependent phenomena in the model to be captured, which conventional equilibria solutions would not do. Frequency domain studies of nonlinear flight mechanics models are currently seldom considered in both industry and academia, so this technique is worth investigating (potentially even more so in the event that future flight dynamics models are extended to represent unsteady aerodynamic phenomena).

These differences have been shown in a simple longitudinal aircraft model example to be prominent at higher angles of attack as the aircraft enters the stall region, which has the potential for undesirable responses such as upsets and loss-of-control. Specifically, the frequency responses of the aircraft with and without a stability-augmentation controller have been assessed. Large discrepancies in gain and phase between the linear and nonlinear frequency responses are seen at low frequencies, where the influence of the phugoid mode is significant. In particular, the extra resonances below the phugoid frequency and the large-amplitude period-2 motion are undetected by the linear model. A controller operating in the period-2 region may perform inadequately if the gain is not sufficiently large, or go completely out of phase and cause much larger responses than predicted if it is operated in the subharmonic resonance region. It should be noted that the polynomial model used in this study was defined to represent the marginal phugoid stability of the full GTM at medium angle of attack, so it is expected that nonlinear behaviors are only observed at low frequencies, and that the model is not particularly representative of the other flight dynamics modes.

Further work can apply the same technique on the full GTM, in which nonlinearity plays a very significant role in its upset dynamics [7]. An analysis of an established controller for the GTM, such as the one developed by Crespo [24] can also be done. This is a gain-scheduled, maneuver-demand, linear-quadratic-regulator controller, in which frequency-domain consideration is not a design driver. The time-domain response of this controller has been studied in detail using AUTO [10]. The techniques presented in this paper are well suited to expand the analysis in [10], especially to determine whether the undesirable attractors become stable isolas that remain within the aircraft operating region.

References

1. Carroll, J.V. and R.K. Mehra, *Bifurcation Analysis of Nonlinear Aircraft Dynamics.* Journal of Guidance, Control, and Dynamics, 1982. **5**(5): p. 529-536.
2. Goman, M.G., G.I. Zagainov, and A.V. Khramtsovsky, *Application of Bifurcation Methods to Nonlinear Flight Dynamics Problems.* Progress in Aerospace Sciences, 1997. **33**(9-10): p. 539-586.
3. Sinha, N., *Applications of Bifurcation Methods to F-18/HARV Open-loop Dynamics in Landing Configuration.* Defence Science Journal, 2002. **52**(2): p. 103-115.
4. Guicheteau, P., *Bifurcation theory: a tool for nonlinear flight dynamics.* Philosophical Transactions of the Royal Society of London. Series A: Mathematical, Physical and Engineering Sciences, 1998. **356**(1745): p. 2181-2201.
5. Avanzini, G. and G.d. Matteis, *Bifurcation Analysis of a Highly Augmented Aircraft Model.* Journal of Guidance, Control, and Dynamics, 1997. **20**(4): p. 754-759.
6. Macmillen, F.B.J. and J.M.T. Thompson, *Bifurcation analysis in the flight dynamics design process? A view from the aircraft industry.* Philosophical Transactions of the Royal Society of London. Series A: Mathematical, Physical and Engineering Sciences, 1998. **356**(1745): p. 2321-2333.
7. Richardson, T., M. Lowenberg, M. DiBernardo, and G. Charles, *Design of a Gain-Scheduled Flight Control System Using Bifurcation Analysis.* Journal of Guidance, Control, and Dynamics, 2006. **29**(2): p. 444-453.
8. Kwatny, H.G., J.-E.T. Dongmo, B.-C. Chang, G. Bajpai, M. Yasar, and C. Belcastro, *Nonlinear Analysis of Aircraft Loss of Control.* Journal of Guidance, Control, and Dynamics, 2013. **36**(1): p. 149-162.
9. Gill, S.J., M.H. Lowenberg, S.A. Neild, B. Krauskopf, G. Puyou, and E. Coetzee, *Upset Dynamics of an Airliner Model: A Nonlinear Bifurcation Analysis.* Journal of Aircraft, 2013. **50**(6): p. 1832-1842.
10. Gill, S.J., M.H. Lowenberg, S.A. Neild, L.G. Crespo, B. Krauskopf, and G. Puyou, *Nonlinear Dynamics of Aircraft Controller Characteristics Outside the Standard Flight Envelope.* Journal of Guidance, Control, and Dynamics, 2015. **38**(12): p. 2301-2308.
11. Nayfeh, A.H. and D.T. Mook, *Nonlinear Oscillations*. Nonlinear Oscillations. 1979, New York: Wiley.
12. Wagg, D. and S. Neild, *Nonlinear vibration with control : for flexible and adaptive structures*. Second edition. ed. Solid mechanics and its applications, 0925-0042 ; volume 218. 2015, Cham: Springer.
13. Holmes, P.J. and D.A. Rand, *The bifurcations of Duffing's equation: An application of catastrophe theory.* Journal of Sound and Vibration, 1976. **44**(2): p. 237-253.
14. Bennett, J.A. and J.G. Eisley, *A multiple degree-of-freedom approach to nonlinear beam vibrations.* AIAA Journal, 1970. **8**(4): p. 734-739.
15. Xia, M. and Q. Sun, *Jump phenomena of rotational angle and temperature of NiTi wire in nonlinear torsional vibration.* International Journal of Solids and Structures, 2015. **56-57**: p. 220-234.
16. Benedettini, F., G. Rega, and R. Alaggio, *Non-linear oscillations of a four-degree-of-freedom model of a suspended cable under multiple internal resonance conditions.* Journal of Sound and Vibration, 1995. **182**(5): p. 775-798.
17. Rega, G. and F. Benedettini, *Planar non-linear oscillations of elastic cables under subharmonic resonance conditions.* Journal of Sound and Vibration, 1989. **132**(3): p. 367-381.
18. Jacobson, S., R. Britt, D. Freim, and P. Kelly, *Residual pitch oscillation (RPO) flight test and analysis on the B-2 bomber*, in *39th AIAA/ASME/ASCE/AHS/ASC Structures, Structural Dynamics, and Materials Conference and Exhibit*. 1998.
19. Baghdadi, N.M., M.H. Lowenberg, and A.T. Isikveren, *Analysis of Flexible Aircraft Dynamics Using Bifurcation Methods.* Journal of Guidance, Control, and Dynamics, 2011. **34**(3): p. 795-809.
20. Mehra, R. and R. Prasanth, *Bifurcation and limit cycle analysis of nonlinear pilot induced oscillations*, in *23rd Atmospheric Flight Mechanics Conference*. 1998.
21. Gránásy, P., P.G. Thomasson, C.B. Sørensen, and E. Mosekilde, *Non-linear flight dynamics at high angles-of-attack.* The Aeronautical Journal (1968), 1998. **102**(1016): p. 337-344.
22. Coetzee, E., B. Krauskopf, and M. Lowenberg. *The dynamical systems toolbox: Integrating AUTO into Matlab*. in *16th US National Congress of Theoretical and Applied Mechanics*. 2010. State College, Pennsylvania.
23. Doedel, E. *AUTO-07P, Continuation and Bifurcation Software for Ordinary Differential Equations, Ver. 07P*. 2007 [cited 2019 19/11]; Available from: http://www.macs.hw.ac.uk/~gabriel/auto07/auto.html
24. Crespo, L., S. Kenny, D. Cox, and D. Murri, *Analysis of Control Strategies for Aircraft Flight Upset Recovery*, in *AIAA Guidance, Navigation, and Control Conference*. 2012.